

Regularized autoregressive modeling and its application to audio signal reconstruction

Ondřej Mokřý, Pavel Rajmic

Abstract—Autoregressive (AR) modeling is invaluable in signal processing, in particular in speech and audio fields. Attempts in the literature can be found that regularize or constrain either the time-domain signal values or the AR coefficients, which is done for various reasons, including the incorporation of prior information or numerical stabilization. Although these attempts are appealing, an encompassing and generic modeling framework is still missing. We propose such a framework and the related optimization problem and algorithm. We discuss the computational demands of the algorithm and explore the effects of various improvements on its convergence speed. In the experimental part, we demonstrate the usefulness of our approach on the audio declipping and dequantization problems. We compare its performance against state-of-the-art methods and demonstrate the competitiveness of the proposed method in declipping musical signals, and its superiority in declipping speech. The evaluation includes a heuristic algorithm of generalized linear prediction (GLP), a strong competitor which has only been presented as a patent and is new in the scientific community.

Index Terms—autoregression, regularization, inverse problems, audio declipping, proximal splitting methods, sparsity

I. INTRODUCTION

AUTOREGRESSIVE (AR) models have been used in a variety of engineering problems. Tasks currently solved with the help of AR modeling include speech coding [1, Sec. 8.2.2], music analysis and coding [2, Ch. 4], and time series prediction in finance [3, Ch. 2], for instance. AR processes have found their use also within control theory [4], where a clear connection to Hankel operators exists [5], [6].

Fitting a signal with an AR process possesses a kind of inverse problem. Thus, where appropriate, it has found its use in reconstruction tasks where data are missing or where data are observed in a degraded form. In its simplest form, the AR fitting of a signal can be understood as a denoiser—the noise is identified with the residual error. A more complicated application example is the time series extrapolation or interpolation of missing segments of audio [7]. In some inverse problems, the prior knowledge about the signal can consist of more than only its AR nature. In such advanced cases, however, a need often arises to regularize or constrain the signal itself or even the AR coefficients. Common AR fitting algorithms are not suitable to cope with such augmented situations.

The contribution of this article is twofold. First, it presents general models which, beside common AR assumptions, allow additional regularization terms, and offers related numerical algorithms. Second, the theory is validated on audio declipping and dequantization problems.

O. Mokřý and P. Rajmic are with the SPLab at the Faculty of Electrical Engineering and Communication, Brno University of Technology, Czech Republic. E-mail: ondrej.mokry@vut.cz, pavel.rajmich@vut.cz,

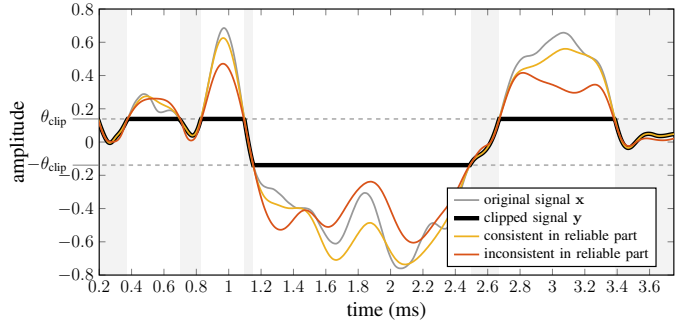


Fig. 1. Illustration of audio clipping and of the consistency property of the declipping solutions; adapted from [10].

A. Audio inverse problems

Audio inpainting, declipping and dequantization are popular signal recovery tasks. In audio inpainting, signal samples are missing, and the inverse problem consists in reconstructing (i.e., estimating) them. Within an optimization framework, which is the most widely used recovery approach, this can be formulated as

$$\min_{\mathbf{x}} f(\mathbf{x}) \quad \text{s.t.} \quad \mathbf{x} \in \Gamma_{\text{inp}} = \{\mathbf{x} \in \mathbb{R}^N \mid \mathbf{M}_R \mathbf{x} = \mathbf{M}_R \mathbf{y}\}. \quad (1)$$

In this problem, a signal \mathbf{x} is sought such that it meets the requirements expressed by the penalization function f . At the same time, \mathbf{x} must perfectly fit the observed portion of the signal $\mathbf{y} \in \mathbb{R}^N$. Here, the matrix \mathbf{M}_R represents a mask of the reliable samples in question, effectively performing row selection. The condition $\mathbf{x} \in \Gamma_{\text{inp}}$ is often called the consistency condition [8].

In audio declipping, samples are not completely missing, but, instead, they are observed saturated (clipped), i.e., samples exceeding the dynamic range $[-\theta_{\text{clip}}, \theta_{\text{clip}}]$ are limited in amplitude according to the nonlinear formula [9], [10]

$$y_n = \begin{cases} x_n & \text{for } |x_n| < \theta_{\text{clip}}, \\ \theta_{\text{clip}} \cdot \text{sgn}^+(x_n) & \text{for } |x_n| \geq \theta_{\text{clip}}. \end{cases} \quad (2)$$

Here, $\text{sgn}^+(z)$ returns 1 for $z \geq 0$ and -1 for $z < 0$ [11], and \mathbf{x} is the input signal and \mathbf{y} is its observed counterpart, see an example in Fig. 1. In such a case, the recovery problem reads

$$\min_{\mathbf{x}} f(\mathbf{x}) \quad \text{subject to} \quad \mathbf{x} \in \Gamma_{\text{declip}}, \quad (3)$$

where the consistency set Γ_{declip} corresponds to the element-wise clipping constraints $\pm\theta_{\text{clip}}$:

$$\Gamma_{\text{declip}} = \left\{ \mathbf{x} \in \mathbb{R}^N \mid \begin{array}{l} \mathbf{M}_R \mathbf{x} = \mathbf{M}_R \mathbf{y} \\ \mathbf{M}_H \mathbf{x} \geq \theta_{\text{clip}} \\ \mathbf{M}_L \mathbf{x} \leq -\theta_{\text{clip}} \end{array} \right\}. \quad (4)$$

The respective matrices \mathbf{M}_R , \mathbf{M}_H and \mathbf{M}_L serve to divide the vector \mathbf{x} into the non-clipped part $\mathbf{M}_R\mathbf{x}$ and the samples exceeding θ_{clip} and $-\theta_{\text{clip}}$, respectively [10].

In declipping, more information is available about the signal than in inpainting. Unfortunately, while the restriction $\mathbf{x} \in \Gamma_{\text{inp}}$ in (1) still allows solving it via the use of common AR fitting algorithms, the additional knowledge coded in $\mathbf{x} \in \Gamma_{\text{declip}}$ is not directly transferable into these algorithms, as will also be discussed in the following part.

As the last example, quantization rounds each signal sample to the nearest from a limited number of quantization levels [1]. Several ways to define the quantization levels are available [12]; in the standard case of the mid-riser uniform quantizer, the quantization levels are equally spaced and symmetric around zero. For a word length of w bits per sample (bps), the quantization step is $\Delta = 2^{-w+1}$ and the quantization process follows the equation

$$y_n = \text{sgn}^+(x_n) \cdot \Delta \cdot \left(\left\lfloor \frac{|x_n|}{\Delta} \right\rfloor + \frac{1}{2} \right). \quad (5)$$

For the dequantization inverse problem, (5) induces the consistency set

$$\Gamma_{\text{dequant}} = \{\mathbf{x} \in \mathbb{R}^N \mid \|\mathbf{x} - \mathbf{y}\|_{\infty} < \Delta/2\}. \quad (6)$$

In comparison to both inpainting and declipping, the constraint in recovering the degraded samples is the most narrow; however, this time no reliable samples are available.

B. Autoregressive methods for signal reconstruction

It is clear that any inpainting method can be used for declipping as well by simply ignoring the conditions involving \mathbf{M}_H and \mathbf{M}_L in (4). This is also the case of the Janssen method [13], [14], which is the state-of-the-art for audio inpainting for compact signal gaps of up to 80ms in length [15], [16]. It is a blockwise, iterative approach where in each iteration, the AR coefficients are estimated for a whole block of a signal and then the missing samples are updated according to the model. In the next iteration, the model is re-estimated based on the current solution and the process is repeated in such a manner. Importantly, the iterations involve standard AR estimation only.

The patent [17] proposes a method for audio declipping, referred to as generalized linear prediction (GLP), that builds upon the idea of Janssen. The extension lies in that after each iteration, all samples currently violating the conditions $\mathbf{M}_H\mathbf{x} \geq \theta_{\text{clip}}$, $\mathbf{M}_L\mathbf{x} \leq -\theta_{\text{clip}}$ are flipped around the respective $\pm\theta_{\text{clip}}$ levels. This is quite a heuristic step but it surprisingly leads to an algorithm that is one of the best performing. The flipping operation on the signal, described by the authors as a rectification, forces the consistency in the clipped part. Interestingly, the method is practically ignored by the signal processing community. The algorithm of [17] represents one of the options on how to cope with the clipping consistency, but we emphasize it is purely heuristic; in our article, we will make an effort to formulate the constraints on the signal \mathbf{x} in a rigorous way and make it a part of the modeling task.

Other important AR-based methods for audio inpainting of compact gaps are those based on extrapolating the right- and

left-hand sides of each gap separately; the interpolation task is then solved by crossfading the two extrapolated sequences [18]–[21]. Similarly, Etter [7] proposes to use separate AR models for the two contexts of the gap, but suggests that the two sets of AR parameters be optimized simultaneously. However, neither of these contributions involves any regularization or constraints and, most importantly, the extrapolation-based methods require a long reliable context of the gap, which limits the use cases significantly.

An ARMA approach to modeling time series with sparsity constraints on both the AR and MA coefficients has been presented in [22]. Later, the authors of [23], [24] presented their approach to audio inpainting under the name High-order sparse linear prediction (HOSpLP). As in the follow-up papers [25], [26], the goal is to recover missing samples of speech by using an AR model with sparsity regularization on the AR coefficients.

Importantly, none of the methods mentioned above offers a flexible interconnection between the AR model and the time-domain requirements on the signal. Furthermore, none of the methods is suitable for audio dequantization, where no reliable parts are available to estimate the AR model and the time-domain constraints are essential.

A Bayesian approach to this problem has been pursued by Troughton and Godsill, using the AR model either on the that complements a sinusoidal deterministic component of the signal [27], or as a self-contained model [28]. The work is generalized in [29] to other non-linear distortions.

The area of signal reconstruction has not been ignored by the advances in deep learning. In particular, declipping and inpainting have been treated by different deep models [30]–[33]. In the context of autoregression, three approaches should be mentioned: First, the popular WaveNet [34] has a conceptual connection with AR modeling, since the generation of signal samples is conditional, given the preceding samples. Second, the AR-Net [35] represents an equivalent description of the AR model, but from the perspective of neural networks. In particular, the AR coefficients are treated as network parameters and optimized using the back-propagation algorithm. This approach also allows regularizing the coefficients by simply adding terms to the loss function. As an example, the authors of [35] mention sparsity, creating a connection with the HOSpLP framework [23]. Finally, Mezza et al. propose a hybrid technique which employs an AR model in parallel with a neural network modeling the residual [36]. However, none of the approaches offers to *constrain the time-domain signal* and direct applications to audio signal reconstruction is missing.

C. Our contribution

Inspired by the success of the heuristic GLP approach that can apply simple constraints in the time domain, and HOSpLP that regularizes the AR coefficients estimation with their sparsity, we propose a general framework that enables regularizing/constraining the time-domain and AR-domain estimation simultaneously. Our formulation stems from a theoretical foundation and, compared to the above mentioned ad-hoc

solutions, it offers an optimization framework, allowing the use of standard proximal algorithms. This way, the framework can be straightforwardly applied to a much wider range of problems than the experimental part actually presents.

The rest of the paper is organized as follows: An overview of the AR model is introduced in Sec. II, together with its regularized variant. An algorithm to solve the task is developed in Sec. III. Sec. IV demonstrates the suitability of the proposed method for the problems of audio declipping and dequantization; the performance of the discussed approaches is compared with that of other optimization-based methods. Effects of different parameters of the proposed model and of the algorithm are also presented. Appendices A to D present supplementary material.

II. AUGMENTING THE AUTOREGRESSIVE MODEL

An autoregressive process of order p is a discrete-time stochastic process $\{X_n \mid n = 0, \pm 1, \pm 2, \dots\}$ defined by the equation

$$X_n + a_2 X_{n-1} + \dots + a_{p+1} X_{n-p} = E_n, \quad \forall n, \quad (7)$$

where $\{E_n\}$ is a zero-mean white noise process with variance $\sigma^2 > 0$ [37, Def. 3.1.2]. In the source-filter signal model, (7) represents the process of passing the excitation noise $\{E_n\}$ through an all-pole filter with coefficients a_1, a_2, \dots, a_{p+1} , where $a_1 = 1$ is assumed without loss of generality [2, Ch. 4].

In terms of real-world signal modeling, (7) can be reformulated for a particular observation $\mathbf{x} \in \mathbb{R}^N$ as

$$\sum_{i=1}^{p+1} a_i x_{n+1-i} = e_n, \quad a_1 = 1, \quad n = 1, \dots, N+p. \quad (8)$$

The vector \mathbf{x} is zero-padded to its new length $N+p$ such that (8) is correctly defined. The definition in (8) is in close relationship with linear convolution and in accordance with the convention of the `lpc` function in Matlab. From the perspective of model fitting, the vector $\mathbf{e} \in \mathbb{R}^{N+p}$ is called the *residual error* [1, Sec. 8.2.2]. Given the observed signal \mathbf{x} and the order p , the AR model parameters are estimated by

$$\arg \min_{\mathbf{a}} \frac{1}{2} \|\mathbf{e}(\mathbf{a}, \mathbf{x})\|^2. \quad (9)$$

In (9), we denote $\mathbf{a} = [1, a_2, a_3, \dots, a_{p+1}]^T$, and $\mathbf{e} = [e_1, e_2, \dots, e_{N+p}]^T$ is defined in (8) as a function of both the signal \mathbf{x} and the coefficients \mathbf{a} . This can effectively be solved, for example, by using the autocorrelation method and the Levinson-Durbin algorithm [38], [39]. Besides, it will be later useful to rewrite the error $\mathbf{e}(\mathbf{a}, \mathbf{x})$ in matrix forms as

$$\mathbf{e} = \mathbf{X}\mathbf{a} = \mathbf{A}\mathbf{x}, \quad (10)$$

where $\mathbf{X} \in \mathbb{R}^{(N+p) \times (p+1)}$ and $\mathbf{A} \in \mathbb{R}^{(N+p) \times N}$ are Toeplitz-structured,

$$\mathbf{A} = \begin{bmatrix} 1 & & & & 0 \\ a_2 & 1 & & & \\ \vdots & a_2 & \ddots & & \\ a_{p+1} & \vdots & & 1 & \\ & a_{p+1} & & a_2 & \\ & & \ddots & \vdots & \\ \mathbf{0} & & & a_{p+1} & \end{bmatrix}, \quad \mathbf{X} = \begin{bmatrix} x_1 & & & & 0 \\ x_2 & x_1 & & & \\ \vdots & x_2 & \ddots & & \\ x_N & \vdots & & x_1 & \\ & x_N & & x_2 & \\ & & \ddots & \vdots & \\ \mathbf{0} & & & x_N & \end{bmatrix}. \quad (11)$$

We define the regularized autoregressive model using an optimization formulation as follows:

$$\arg \min_{\mathbf{a}, \mathbf{x}} \left\{ Q(\mathbf{a}, \mathbf{x}) = \frac{1}{2} \|\mathbf{e}(\mathbf{a}, \mathbf{x})\|^2 + \lambda_C f_C(\mathbf{a}) + \lambda_S f_S(\mathbf{x}) \right\}, \quad (12)$$

where we assume $\lambda_C, \lambda_S \geq 0$, and f_C, f_S are (preferably) convex lower semicontinuous functions, where the subscripts indicate the connection to the coefficients or the signal. The idea behind (12) is that the AR nature of the signal is preserved by minimizing the residual error as in (9) but, at the same time, possible priors on the AR coefficients \mathbf{a} and the signal \mathbf{x} are incorporated via the functions f_C and f_S , respectively.

The audio inpainting task, as originally presented in [13], corresponds to problem (12) with $f_C = 0$ and f_S being the indicator function of the set Γ_{inp} of feasible signals; see also (1). In such a situation, the hard constraints $\mathbf{M}_R \mathbf{x} = \mathbf{M}_R \mathbf{y}$ can be directly incorporated in the noise-minimization term using a complementary matrix $\bar{\mathbf{M}}_R$ selecting the missing samples: Decomposing $\mathbf{e}(\mathbf{a}, \mathbf{x}) = \mathbf{A}\mathbf{x} = \mathbf{A}\mathbf{M}_R^T \mathbf{M}_R \mathbf{x} + \mathbf{A}\bar{\mathbf{M}}_R^T \bar{\mathbf{M}}_R \mathbf{x}$, we arrive at

$$\arg \min_{\mathbf{a}, \mathbf{x}} \left\{ Q(\mathbf{a}, \mathbf{x}) = \frac{1}{2} \|\mathbf{A}\mathbf{M}_R^T \mathbf{M}_R \mathbf{y} + \mathbf{A}\bar{\mathbf{M}}_R^T \bar{\mathbf{M}}_R \mathbf{x}\|^2 \right\}, \quad (13)$$

where we substituted $\mathbf{M}_R \mathbf{y}$ for $\mathbf{M}_R \mathbf{x}$, expressing the hard constraint. Given \mathbf{a} , this task represents a least-squares problem with $\bar{\mathbf{M}}_R \mathbf{x}$ being the variables, which can be solved more efficiently compared with working directly with (12).

A similar model is the HOSpLP framework for audio inpainting [25], where the coefficient estimation is regularized solely by $f_C(\mathbf{a}) = \|\mathbf{a}\|_1$, or even by a non-convex sparsity penalty [26]. In contrast to (12), HOSpLP further allows utilizing a different norm for the residual \mathbf{e} , which is assumed to be more suitable, e.g., to model voiced speech (in such a case, the source in the source-filter model is a pulse train rather than white noise).

Another reason for the AR model regularization may be numerical stability. We observed that without a regularization of the AR coefficients, the overall objective function and SNR may improve in the course of iterations, but the AR coefficients themselves may grow disproportionately (for example, a difference in the order of 10^4 compared with the ground-truth signal AR coefficients can appear). An extreme case we observed was a failure of the AR model estimation for rare combinations of signals and high model orders. In these cases, the estimation failed due to inversion of a badly conditioned matrix. Using the parameter $\lambda_C > 0$, this numerically undesirable behavior can be controlled.

III. ALGORITHMIC APPROACH

Suppose the functions f_C, f_S are convex; it follows that the problem (12) poses a biconvex optimization, meaning that although (12) as a whole is non-convex, minimizations of $Q(\mathbf{a}, \mathbf{x})$ over \mathbf{a} and over \mathbf{x} separately represent convex problems. Such cases appear frequently in the literature [6], [40], and the problem is typically treated via the Alternate Convex Search (ACS) [41, Sec. 4.2.1].

A. Alternate Convex Search Algorithm

Statements regarding the convergence of the ACS are generally not possible, see also [13, App. B]. Thanks to biconvexity, however, at least the convergence of the objective values can be guaranteed, i.e., of the sequence $\{Q(\mathbf{a}^{(i)}, \mathbf{x}^{(i)}) \mid i = 1, 2, \dots\}$ [41, Thm. 4.5]. However, the limit of the sequence may not be the global minimum of $Q(\mathbf{a}, \mathbf{x})$. Some practical convergence properties can be formulated when the sequence $\{(\mathbf{a}^{(i)}, \mathbf{x}^{(i)})\}$ is contained in a compact set, which could be enforced, for example, by defining f_C, f_S as indicator functions [42], and if both the individual convex sub-problems have unique solutions. Under these assumptions, the ACS sequence has at least one accumulation point and all the accumulation points are stationary points of $Q(\mathbf{a}, \mathbf{x})$ [41, Thm. 4.9, Corr. 4.10], [43, Sec. 4.2]. Such a behavior is reported also in [13, App. B]. Reference [13] presents a relation to the expectation–maximization scheme (EM) which, however, is not accompanied with encouraging convergence properties in a general setup [43, Ch. 5].

In both the sub-problems of minimizing Q over \mathbf{a} and over \mathbf{x} , the other variable is constant, which allows omitting the respective part of the objective function in (12) and simplifying the updates to

$$\mathbf{a}^{(i)} = \arg \min_{\mathbf{a}} \left\{ \frac{1}{2} \|\mathbf{e}(\mathbf{a}, \mathbf{x}^{(i-1)})\|^2 + \lambda_C f_C(\mathbf{a}) \right\}, \quad (14a)$$

$$\mathbf{x}^{(i)} = \arg \min_{\mathbf{x}} \left\{ \frac{1}{2} \|\mathbf{e}(\mathbf{a}^{(i)}, \mathbf{x})\|^2 + \lambda_S f_S(\mathbf{x}) \right\}. \quad (14b)$$

In the following subsections, the ways to solve (14a) and (14b) are discussed. As will be demonstrated, it turns out that the bottleneck is the computational complexity. Therefore, the possibilities of accelerating the ACS procedure will also be discussed.

B. Dealing with the sub-problems

In the convex setting and with nonzero f_C, f_S , the problems (14a) and (14b) can be addressed via proximal splitting methods [42]. Each of the problems consists of a sum of two convex functions: the quadratic AR model error and a possibly non-smooth penalty f_C or f_S . The key concept of the proximal splitting is to reach the global optimum by repetitive minimization using gradients or the so-called proximal operators related to individual summands.

The proximal operator of a function f is another function acting on the same space, defined as $\text{prox}_f(\mathbf{u}) = \arg \min_{\mathbf{v}} \left\{ \frac{1}{2} \|\mathbf{v} - \mathbf{u}\|^2 + f(\mathbf{v}) \right\}$. Among the typical examples is the projection onto a convex set C , which is the proximal operator of the indicator function of the set, ι_C . Another example is the soft thresholding with the threshold γ as the proximal operator of the scaled ℓ_1 norm $\gamma \|\cdot\|_1$. For more examples and background, see e.g. [42], [44, Ch. 6].

Each of the problems (14a) and (14b) can be addressed via the Douglas–Rachford algorithm (DRA) [42, Sec. 4], which requires access to the proximal operators of the two summands involved. In the case of (14), this applies to the quadratic function and either $\lambda_C f_C$ or $\lambda_S f_S$.

We further assume that $\text{prox}_{\lambda_C f_C}(\mathbf{a})$ and $\text{prox}_{\lambda_S f_S}(\mathbf{x})$ are available in an explicit form, which will be the case later in

Section IV (see also Appendix D). To deal with the quadratic model error term, recall the matrix form presented in (10). Then, the proximal operators of $\frac{1}{2} \|\mathbf{e}(\mathbf{a}, \mathbf{x})\|^2$ with respect to \mathbf{a} and \mathbf{x} can simply be expressed as [42, Table I]

$$\text{prox}_{\gamma_C \|\mathbf{e}(\cdot, \mathbf{x})\|^2 / 2}(\mathbf{a}) = (\mathbf{I} + \gamma_C \mathbf{X}^\top \mathbf{X})^{-1} \mathbf{a}, \quad (15a)$$

$$\text{prox}_{\gamma_S \|\mathbf{e}(\mathbf{a}, \cdot)\|^2 / 2}(\mathbf{x}) = (\mathbf{I} + \gamma_S \mathbf{A}^\top \mathbf{A})^{-1} \mathbf{x}. \quad (15b)$$

Here γ_C and γ_S are parameters of the DRA for the respective problems. The underlying structure of the matrices allows an efficient numerical implementation without employing the inverse explicitly—it is based on appending rows to the matrices \mathbf{X} and \mathbf{A} in (15a) and (15b), respectively, yielding a circulant structure, allowing obtaining the inverses efficiently using the FFT. Importantly, applying these extended proximal operators in solving the problems (14a) and (14b) guarantees reaching the same minimum as with employing (15a) and (15b) directly [45].

Note that further acceleration is achievable by heuristic schemes—an example is the extrapolation of the updates given by (14). These alternatives, as well as a larger evaluation of the properties of the FFT-accelerated DRA in the context of audio declipping, can be found in Appendix A.

The whole ACS is summarized in Algorithm 1, featuring the Janssen audio inpainting [13] as a particular case.

Algorithm 1: ACS solving (12)

```

1 initialize  $\mathbf{x}^{(0)}$ 
2 for  $i = 1, 2, \dots$  do
3   coef. update (14a)
4   define  $\mathbf{X}$  given  $\mathbf{x}^{(i-1)}$  // (11)
5   if  $\lambda_C = 0$  then
6      $\mathbf{a}^{(i)} = [1; \mathbf{X}(:, 2:\text{end})^\top \mathbf{X}(:, 1)]$  //  $\text{lpc}(\mathbf{x}^{(i)})$ 
7   else
8     define  $\text{prox}_{\gamma_C \lambda_C f_C}(\mathbf{a})$  // Appendix D
9      $\text{prox}_{\gamma_C \|\mathbf{e}(\cdot, \mathbf{x})\|^2 / 2}(\mathbf{a}) = (\mathbf{I} + \gamma_C \mathbf{X}^\top \mathbf{X})^{-1} \mathbf{a}$  // (15a)
10     $\mathbf{a}^{(i)} = \text{DRA}(\text{prox}_{\gamma_C \|\mathbf{e}(\cdot, \mathbf{x})\|^2 / 2}, \text{prox}_{\gamma_C \lambda_C f_C}, \text{params})$ 
11  end
12  extrapolate the estimate  $\mathbf{a}^{(i)}$  // Appendix A
13  signal update (14b)
14  define  $\mathbf{A}$  given  $\mathbf{a}^{(i)}$  // (11)
15  if inpainting, consistent then
16    set  $\overline{\mathbf{M}}_R \mathbf{x}^{(i)} = \overline{\mathbf{M}}_R \mathbf{y}$ 
17    set  $\overline{\mathbf{M}}_R \mathbf{x}^{(i)} = -(\mathbf{A} \overline{\mathbf{M}}_R^\top)^\dagger \mathbf{A} \overline{\mathbf{M}}_R^\top \overline{\mathbf{M}}_R \mathbf{y}$  // (13)
18  else
19    define  $\text{prox}_{\gamma_S \lambda_S f_S}(\mathbf{x})$  // Appendix D
20     $\text{prox}_{\gamma_S \|\mathbf{e}(\mathbf{a}, \cdot)\|^2 / 2}(\mathbf{x}) = (\mathbf{I} + \gamma_S \mathbf{A}^\top \mathbf{A})^{-1} \mathbf{x}$  // (15b)
21     $\mathbf{x}^{(i)} = \text{DRA}(\text{prox}_{\gamma_S \|\mathbf{e}(\mathbf{a}, \cdot)\|^2 / 2}, \text{prox}_{\gamma_S \lambda_S f_S}, \text{params})$ 
22  end
23  extrapolate the estimate  $\mathbf{x}^{(i)}$  // Appendix A
24  perform line search // Appendix A
25 end
```

Line 6 of Algorithm 1 uses Matlab notation for the selection of matrix rows and columns. The formula itself can be derived from (9) by substituting $\mathbf{e} = \mathbf{X}\mathbf{a}$, see (10) and (11), fixing

$\mathbf{a}_1 = 1$ and solving the resulting least-squares problem using the pseudoinverse, denoted as $(\cdot)^+$. Similarly, line 17 presents the explicit solution to the least-squares problem (13).

Note that in practice, the proximal operators on lines 8 and 19 do not depend on the current value of $\mathbf{x}^{(i-1)}$ and $\mathbf{a}^{(i)}$, respectively. Also note that the acceleration steps on lines 12, 23 and 24 are optional and heuristic.

IV. EXPERIMENTS AND RESULTS

This section mostly concerns the audio declipping task; the application to audio dequantization is discussed in Sec. IV-F.

The AR-based declipping task can be posed as an optimization problem in the form of (12):

$$\arg \min_{\mathbf{a}, \mathbf{x}} \left\{ \frac{1}{2} \|\mathbf{e}(\mathbf{a}, \mathbf{x})\|^2 + \lambda_C \|\mathbf{a}\|_1 + \lambda_S d_{\Gamma_{\text{declip}}}(\mathbf{x})^2 / 2 \right\}, \quad (16)$$

where $d_{\Gamma_{\text{declip}}}(\mathbf{x}) = \|\mathbf{x} - \text{proj}_{\Gamma_{\text{declip}}}(\mathbf{x})\|_2$ denotes the distance of \mathbf{x} from the set of feasible signals Γ_{declip} . Letting $\lambda_S = \infty$ allows the problem (16) to cover the *consistent* declipping solution, yielding the hard constraint $\mathbf{x} \in \Gamma_{\text{declip}}$ as in (3) (see also Appendix D). In the case of $0 < \lambda_S < \infty$, the solution is allowed to be *inconsistent* (see also Fig. 1).

Furthermore, we compare the solution to our problem (16) with two reduced approaches. The first one is the inpainting strategy from the original work of Janssen et al. [13], treating the clipped samples as completely missing with no clipping-related constraints. The second one is the generalized linear prediction (GLP), described in Sec. I-B, which heuristically modifies Janssen's original approach to declipping [17].

Following on the HOSpLP framework [25], we allow the regularization of the AR model coefficients via the ℓ_1 norm by setting $\lambda_C > 0$ in (16). The same regularization is applied in the inpainting and GLP cases, where the AR model update (14a) does not differ from the declipping case.

To deal with long (and non-stationary) signals, the proposed regularized AR model is used and estimated frame-wise. The same as in the seminal inpainting paper [46], we use the rectangular window to divide the input signal into overlapping segments of length w ; after optimization, the final overlap-add synthesis is done with the sine window to enable smooth transition between adjacent frames.

Throughout this section, the quality of the declipped audio signal is assessed using the signal-to-distortion ratio (SDR). For the original (undegraded) signal \mathbf{y} and a reconstruction $\hat{\mathbf{x}}$, SDR in decibels is computed as

$$\text{SDR}(\mathbf{y}, \hat{\mathbf{x}}) = 10 \log_{10} \frac{\|\mathbf{y}\|^2}{\|\mathbf{y} - \hat{\mathbf{x}}\|^2}. \quad (17)$$

As in the declipping survey [9], the perceived quality of the signal is additionally evaluated using the PEMO-Q [47] and PEAQ metrics [48], [49]. Both of them predict the subjective difference of the signals \mathbf{y} and $\hat{\mathbf{x}}$ in terms of the objective difference grade (ODG), which ranges from -4 (very annoying impairment) to 0 (imperceptible difference).

The test signals are also taken from the survey [9], i.e., musical recordings sampled at 44.1 kHz and cropped to a length of around 7 seconds are used, originally based on the EBU SQAM database [50].

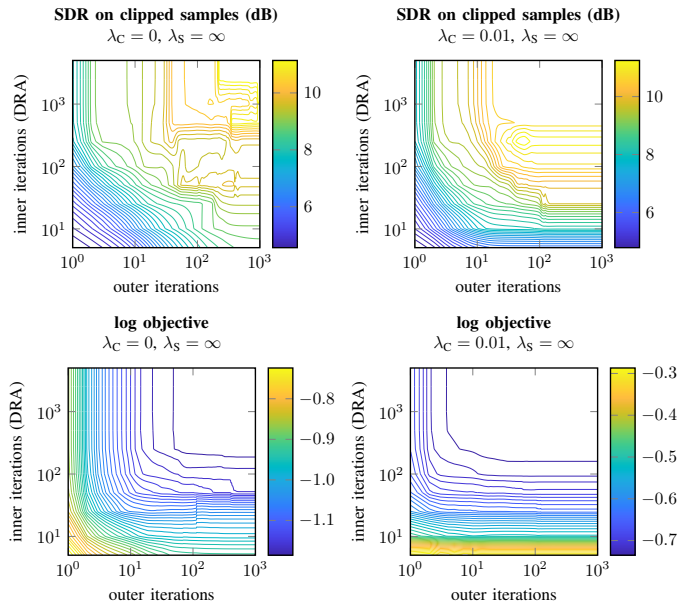


Fig. 2. Trade-off between the count of inner and outer iterations. The problem being solved is the consistent declipping of a single signal frame, i.e., problem (16) with $\lambda_S = \infty$ and varying λ_C . The signal segment length is 2048 samples, the model order is $p = 512$. For reference, the SDR of the clipped signal is 4.3 dB.

In the following subsections IV-A to IV-C, preliminary experiments focused on various aspects of the numerical optimization are presented; these are performed on limited subsets of the above described dataset. The main experiment on declipping of musical signals comes in Sec. IV-D, where the methods considered are evaluated against the results of the declipping survey; there, the full set of signals is used. Extension to declipping of speech signals is provided in Sec. IV-E, followed by illustration on the dequantization problem (Sec. IV-F) and a discussion of computational complexity (Sec. IV-G).

A. Trade-off between Outer and Inner Iteration Counts

Since the algorithmic approach proposed in Section III-B involves nested iterations, a natural question arises on the trade-off between the number of iterations of the whole ACS (outer) and the number of iterations of the sub-solver (inner). To examine this trade-off, we perform the declipping of a single signal frame by solving problem (16). For different combinations of the number of inner and outer iterations, the reconstruction quality is measured using the SDR, together with tracking the value of the objective function of (16).

The main conclusion from this experiment is that a sufficient number of both inner and outer iterations is crucial for reaching a low objective value/high SDR. However, from approximately 100 outer and 1000 inner iterations upwards, the result no longer improves. Importantly, the consistent improvement with the number of outer iterations (i.e., along the horizontal axis) suggests that the unknown convergence properties, as discussed in Sec. III-A, are not very limiting, at least in our setup. The last conclusion is that especially in the case of AR model regularization (plots in the right column of

Fig. 2 with $\lambda_C = 0.01$), the number of inner iterations (i.e., the precision in solving sub-problems (14)) is critical.

B. Progression towards ground-truth coefficients?

The previous experiment suggests the suitability of the regularized AR model for audio declipping, since the SDR values indicate that the reconstructed audio resembles the undistorted original. This section aims at answering the subsequent question, whether even the sequence of AR coefficients $\{\mathbf{a}^{(i)}\}$ generated by the ACS converges towards the AR coefficients \mathbf{a}^{true} of the original signal (prior to clipping).

To investigate this subject, a declipping experiment according to (16) is performed, where, in addition to the objective and the SDR, we track the evolution of the (regularized) AR coefficients in the iterations of the ACS. This allows a comparison with the coefficients of the undistorted signal using the norm $\|\mathbf{a}^{(i)} - \mathbf{a}^{\text{true}}\|$.

The results of the experiment are presented in Fig. 3. The conclusion is that it is possible that the AR coefficients converge over iterations—usually the relative difference between iterations decreases, see the last plot in Fig. 3 showing the values of $\|\mathbf{a}^{(i)} - \mathbf{a}^{(i-1)}\| / \|\mathbf{a}^{(i)}\|$. However, it appears that even if the sequence $\{\mathbf{a}^{(i)}\}$ converges, it does not converge to the coefficients of the undamaged signal \mathbf{a}^{true} . This is because the norm of the difference to this *actual* solution (plotted in the third graph) usually does not decrease.

C. Regularization

After demonstrating that the proposed algorithmic approach allows fitting the regularized AR model, the aim is to dig deeper in the declipping application. A common question in regularized inverse problems is the trade-off related to the regularization strength, typically governed by a scalar parameter. In the case of the generic problem (12), or the particular declipping formulation (16), there are two regularization parameters λ_C, λ_S , which may significantly affect the reconstruction quality.

To evaluate the effect of the regularization, an experiment is performed where clipped signals are reconstructed using all three strategies (inpainting, GLP, declipping), for different choices of λ_C and λ_S in the case of the proposed declipping approach. The results, in terms of SDR, are presented in Table I. The observation is that the results are not very sensitive to the choice of λ_S , even though the declipping strategy (i.e., $\lambda_S > 0$) leads to a minor improvement over inpainting or GLP. Regarding λ_C , the choice to regularize the AR coefficients (i.e., $\lambda_C > 0$) also improves the reconstruction quality; however, the regularization must be chosen carefully in order not to be overly strong (see the results for $\lambda_C = 10^{-1}$).

D. Declipping of musical signals

To provide a context for the reconstruction quality reachable by the regularized AR model, our last experiment compares the results with the survey [9]. The same set of 10 musical signals is used and degraded in the same way, i.e., hard-clipped with the clipping level chosen according to a given input SDR (5, 7, 10 and 15 dB).

The order of the regularized AR model is $p = 512$, with the frame length set to $w = 8192$ samples. The inner iterations are solved using the FFT-accelerated DRA with 1 000 iterations, and the ACS algorithm runs for 5 outer iterations with signal extrapolation (see Appendix A-B).

First, the results are evaluated using the SDR, shown in Fig. 4a. More precisely, Fig. 4a shows the ΔSDR values, which are defined as the difference between the SDR of the recovered signal and the input SDR of the clipped signal.

The effect of the regularization of the AR coefficients (λ_C) in the case of inpainting and GLP appears to be rather negative in terms of the quality of the reconstruction. On the other hand, it is beneficial in the case of declipping for input SDR < 15 dB. An important observation is that GLP does *not* perform better than inpainting, and it outperforms declipping only for a very low input SDR. This suggests that if time-domain consistency is essential, the declipping strategy represents a better choice; if computational complexity is the priority, then the inpainting strategy is sufficient. For a lower input SDR, the results are positively affected also by increasing $\lambda_S > 0$.

The overall outcome of the experiment is that compared to the methods tested in the survey [9], the regularized AR model scores among the best and offers an alternative to state-of-the-art methods. However, a significant improvement of the state of the art is not observed.

Furthermore, the regularization of the signal ($\lambda_S > 0$) was expected to be clearly beneficial, but it led to outperforming the other AR-based competitors (inpainting, GLP) for a higher input SDR only. For further discussion on the consistency of the declipped signals, see Appendix B.

As the final part of this evaluation, Fig. 5 illustrates a statistical significance test using the Wilcoxon signed rank test [51]. The test compares the results of all pairs of methods. The right-tailed hypothesis test was configured such that rejection of the null hypothesis (p -value smaller than 0.05) suggests higher median of the first method from the couple under test. As an example, the analysis reveals that all the proposed declipping cases outperform the GLP with model regularization ($\lambda_C > 0$). The declipping case with $\lambda_C = 10^{-5}$ and $\lambda_S = \infty$ outperforms also the unmodified GLP, but with p -value close to the decision level. In summary, the proposed methods significantly outperform 10 out of the 16 baselines. Statistical tests for other values of the input SDR are presented at the accompanying GitHub page (see the link in Sec. IV-H).

E. Speech declipping

To strengthen the generality of the proposed framework, an extension of the previous comparison focuses on declipping of speech. This experiment uses a subset of 20 signals from the dataset [52] (2 speakers, 1 male and 1 female, 10 signals each). The original sounds represent clean speech excerpts with the length ranging from 1.6 to 3.8 seconds, with no significant portions of silence, sampled at 48 kHz.

The hyperparameters of the reconstruction were adapted to speech, namely the AR model order $p = 256$ and frame length $w = 2048$ samples (approx. 43 ms) were used. Three baselines were selected from the methods tested in the survey [9] and applied with the frame length of $w = 2048$ samples.

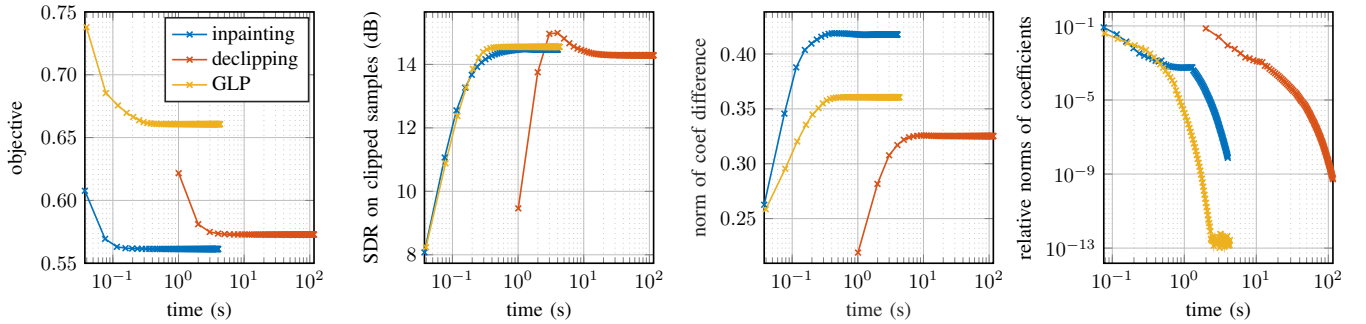


Fig. 3. Analysis of convergence of the three main competitors towards both the clean signal and the ground-truth AR coefficients. In this particular case, a 2048-sample-long realization of an AR process of the order $p = 128$ was used as the ground-truth signal and clipped at 0.2 times the peak value (corresponding to an SDR of 4.6 dB on the clipped samples). For reconstruction, we set $\lambda_C = 0.1$ and $\lambda_S = \infty$ (i.e., declipping in its consistent variant). All three algorithms run for 100 outer iterations and 1 000 inner iterations of the (non-accelerated) DRA. Note that the objective functions (the first graph) are in general different for different algorithms due to the choices of the parameters λ_C, λ_S .

TABLE I
MEAN SDR (dB) FROM 10 SIGNALS, EACH INITIALLY DEGRADED BY CLIPPING AT AN INPUT SDR OF 10 dB. THE PARAMETERS USED IN THE RECONSTRUCTION ARE $w = 2048$, $p = 512$, 10 OUTER ITERATIONS AND 1 000 INNER ITERATIONS. FOR EACH ALGORITHM (DECLIPPING, GLP, INPAINTING), THE MAXIMAL VALUE (PRIOR TO ROUNDING) IS HIGHLIGHTED.

| | $\lambda_C = 0$ | $\lambda_C = 10^{-6}$ | $\lambda_C = 10^{-5}$ | $\lambda_C = 10^{-4}$ | $\lambda_C = 10^{-3}$ | $\lambda_C = 10^{-2}$ | $\lambda_C = 10^{-1}$ |
|----------------------------------|-----------------|-----------------------|-----------------------|-----------------------|-----------------------|-----------------------|-----------------------|
| declipping, $\lambda_S = \infty$ | 22.9 | 23.5 | 23.5 | 23.7 | 24.3 | 23.1 | 19.1 |
| declipping, $\lambda_S = 100$ | 22.9 | 23.5 | 23.5 | 23.7 | 24.3 | 23.1 | 19.1 |
| declipping, $\lambda_S = 10$ | 22.9 | 23.5 | 23.6 | 23.7 | 24.3 | 23.0 | 18.9 |
| declipping, $\lambda_S = 1$ | 22.4 | 23.1 | 23.1 | 23.3 | 23.8 | 22.1 | 18.0 |
| GLP | 22.4 | 22.4 | 22.4 | 22.5 | 22.6 | 21.9 | 18.0 |
| inpainting | 23.4 | 23.2 | 23.3 | 23.5 | 23.9 | 22.1 | 17.7 |

For speech-specific evaluation, the Short-Time Objective Intelligibility (STOI) is employed, ranging from -1 to 1 and providing an intelligibility-based comparison of a test signal to a reference signal [53], [54]. Besides, Virtual Speech Quality Objective Listener (ViSQOL) is used to assess psychoacoustical similarity of speech signals. This model uses two scores: the mean opinion score (MOS) and the neurogram similarity index measure (NSIM) [55]–[57].

The results in terms of Δ SDR and STOI are shown in Fig. 6. Regarding Δ SDR and the proposed methods, both consistent and inconsistent declipping with ACS outperform the inpainting and GLP cases. Positive effect of the AR model regularization ($\lambda_C > 0$) is also pronounced. Importantly, the proposed AR-based declipping also outperforms the baselines with the only exception of A-SPADE at input SDR of 5 dB. It is worth noting that SSPEW was selected as the best performing from Sec. IV-D; however, it does not reach the results of A-SPADE in the case of speech.¹ Regarding STOI, the differences are subtle and the effect of λ_C appears insignificant. On the other hand, the proposed methods outperform the baselines for all clipping levels. Equivalent outcomes to those of STOI stem from the MOS and NSIM metrics, which are not displayed.

F. Audio dequantization

The audio dequantization task can also be formalized within the framework of regularized AR modeling in the form of

¹This can be attributed to the fact that SSPEW exploits the persistence properties of sounds, which is significant in music but only concerns voiced segments of speech in a limited manner.

problem (16). The difference to audio declipping lies only in the consistency set: Γ_{declip} is now replaced by Γ_{dequant} as defined in (6). The same as above, $\lambda_S = \infty$ corresponds to the consistent case and $0 < \lambda_S < \infty$ to the inconsistent case.

Fig. 7 shows an illustrative reconstruction of a quantized piano recording. The clean recording is taken from the dataset described in Sec. IV-D and the uniform quantization from (5) is used with 5 bits per sample, corresponding to a total of 32 quantization levels with a step of $\Delta = 2^{-5+1} = 0.0625$.

The plot shows a detail of the waveform of the clean signal, the reference reconstruction by the sparsity-based S-SPADQ algorithm [11] and, finally, the proposed regularized AR approach, with different regularization strengths.

The example shows a variety of reconstructions depending on both the signal consistency (values of λ_S) and AR model regularization (values of λ_C). Interestingly, from the two possibly inconsistent solutions ($\lambda_S = 0.1$), we observe actual breaking of the consistency constraints only in the case of the regularized AR model ($\lambda_C = 0.1$).

G. Computational complexity

Regarding the computational demands of the proposed methods, several insights can be reported:

- The most demanding is the iterative solution of sub-problems (14a) (if $\lambda_C > 0$) and (14b) (see also Sec. III-B). From (11) and (15), we observe that the computation is dominated by matrix manipulations, where the dimensions grow with both the signal/window length N and model order p . More precisely, the complexity of

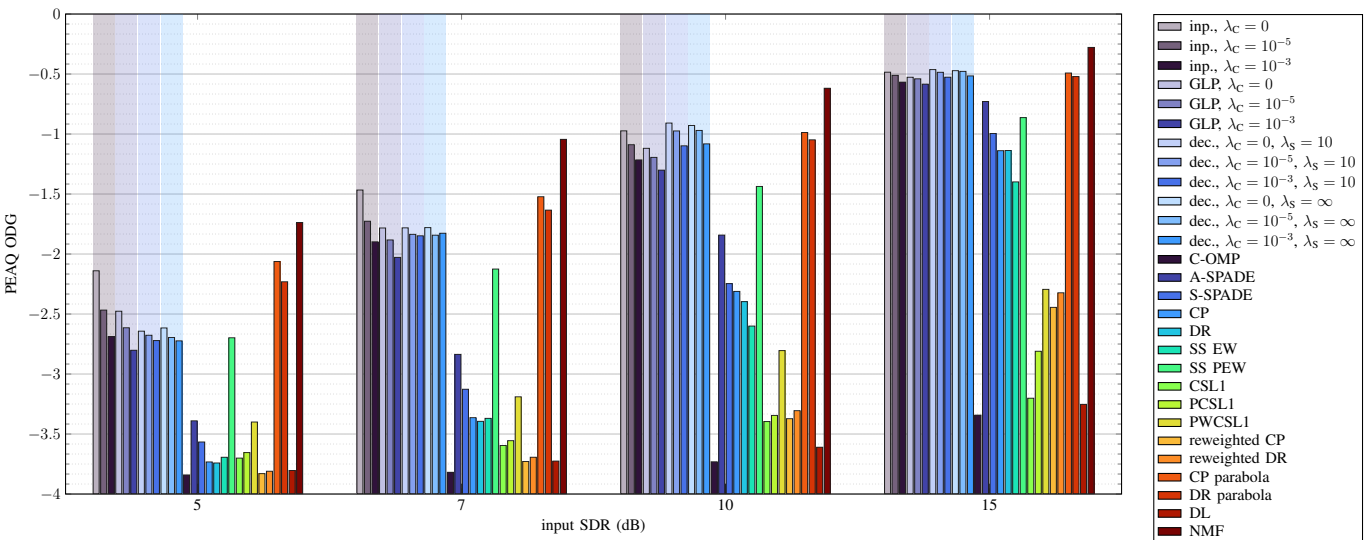
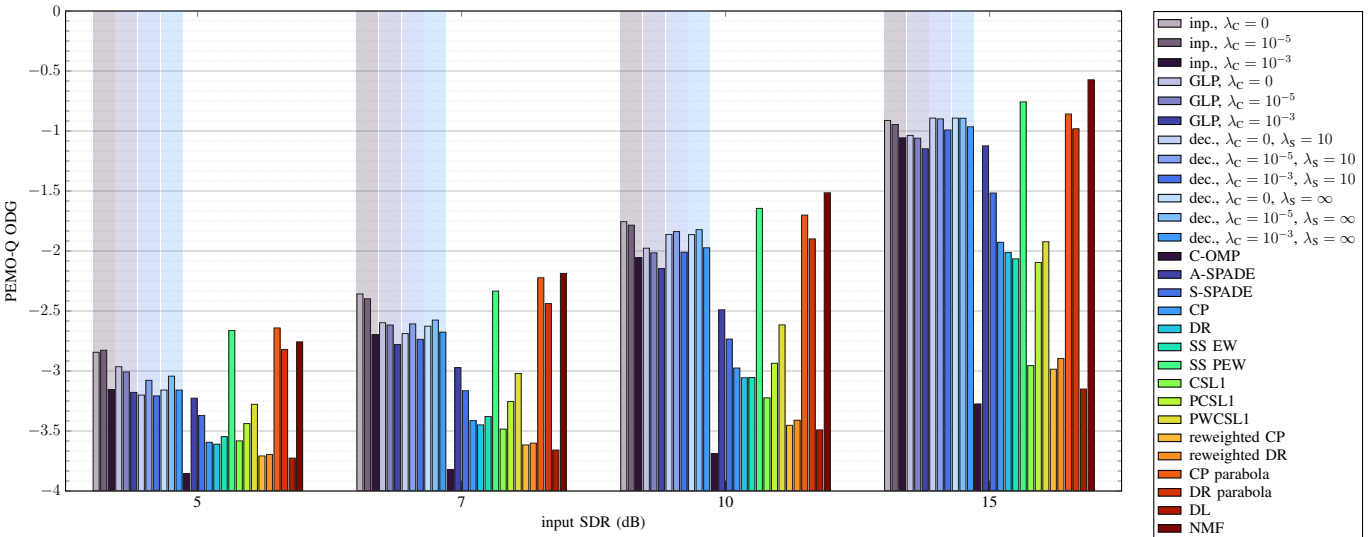
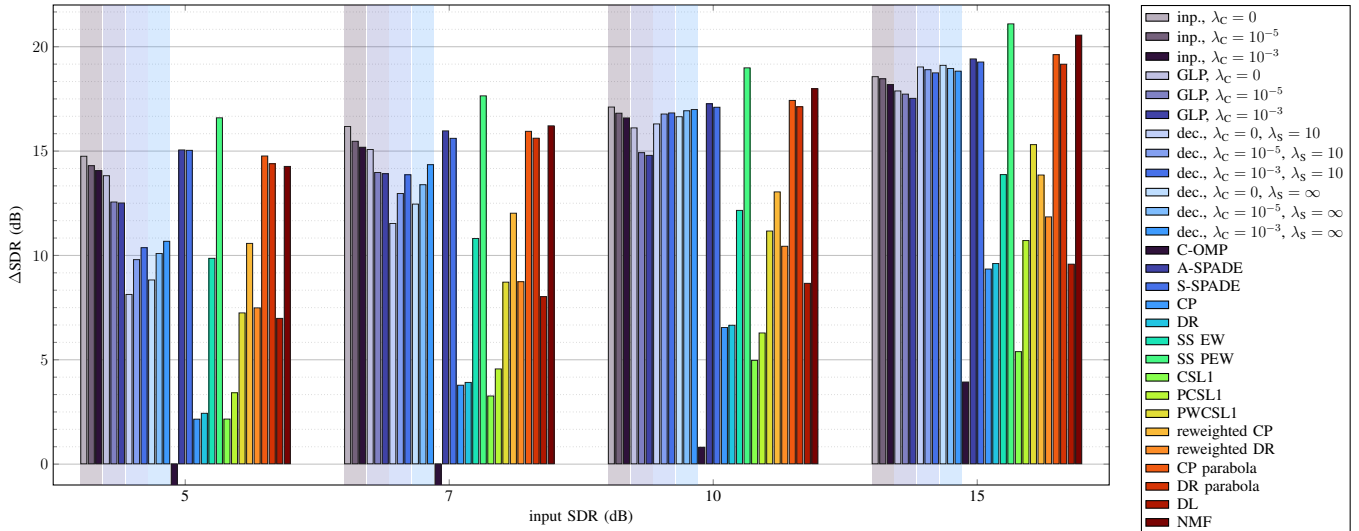


Fig. 4. Comparison of the regularized AR model with the methods from the survey [9]. Results of the methods based on the AR model, treated in this article, are indicated with a background color.

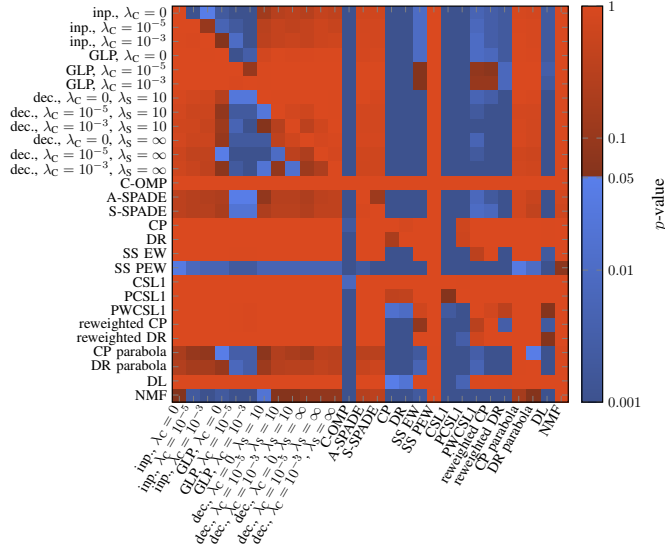
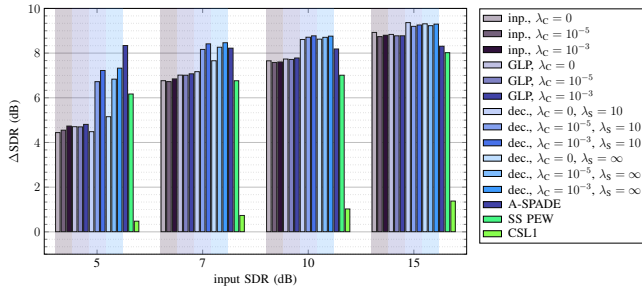
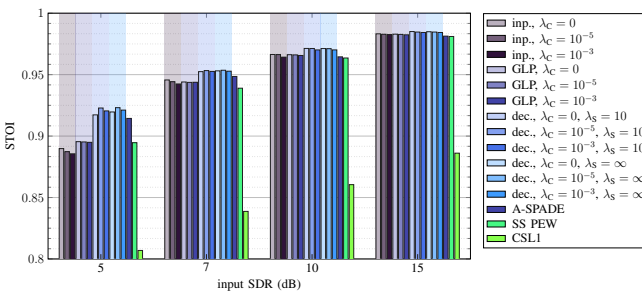


Fig. 5. Illustration of testing the statistical hypothesis on the Δ SDR results for the case of input SDR 10 dB (i.e., third group of columns in Fig. 4a). Each entry of the matrix represents a comparison of the method on the vertical axis to the method on the horizontal axis. Entries with p -value < 0.05 suggest superiority of the corresponding method on the vertical axis and are colored in shades of blue. Failure to reject the null hypothesis (i.e., possible equality of the medians) is colored in red.



(a) comparison in terms of Δ SDR, i.e. the improvement of SDR over the clipped signal



(b) comparison in terms of STOI (note the cropped y-axis)

Fig. 6. The proposed regularized AR model is compared with selected methods from the survey [9], here on a speech dataset. The color-coding follows the experiment on musical signals in Sec. IV-D and Fig. 4.

matrix inversion (needed every outer iteration) is $O(N^3)$ in the signal update (14b) and $O(p^3)$ in the model update (14a).

- In practical cases it holds $p \ll N$, therefore the model-related sub-problem (14a) is numerically less demanding compared to the signal-related sub-problem (14b).

- In the case of inpainting and GLP, the signal estimation is done using matrix inversion, where the matrix size grows with the signal/window length and the number of missing/clipped samples (which is in an inverse relationship with the clipping threshold θ_{clip} and with the input SDR).
- On the other hand, the computational load of the signal estimation (14b) in the case of declipping with ACS does not depend on the number of degraded samples.

To evaluate the complexity numerically, Fig. 8 complements the results of Fig. 4 in terms of elapsed times. While regularized declipping steadily requires above two minutes of computation per a second of audio, inpainting and GLP become faster with a decreasing number of degraded audio samples.

To compare the observations with the reference methods, we provide several comments taken from [9, Sec. V.D]: The NMF method, as one of the best performing, takes on average 30 minutes (1 800 s) per second of input audio; on the other hand, SS PEW takes only around 120 s while also scoring high values of both SDR and ODG. The fastest methods considered in [9] were DR and CP with 20 seconds of computation per one second of input audio.

Further comments and analysis are provided in Appendix C.

H. Software, data & reproducible research

Our software and supplementary materials (figures, listening examples) are available through the link <https://github.com/ondrejmkry/RegularizedAutoregression>. We run the codes using Matlab R2025b.

To obtain results via the basic Janssen method (i.e., effectively audio inpainting) we used parts of the SMALLbox [46]. The same applies to the GLP method [17], whose fundamental step coincides with that of the Janssen method. The FFT-based acceleration of the Douglas–Rachford algorithm was taken from [45]. When comparing our results with those of the reference methods from the survey [9], we took directly the reported and publicly available signals from the accompanying repository https://github.com/rajmic/declipping2020_codes.

V. CONCLUSION

We have developed a comprehensive and general framework alongside its associated optimization problem and algorithm which encompasses the previous attempts to enhance the basic popular AR model. The framework allows constraining the signal values in the time domain and/or regularizing the AR coefficients. One of the novelties of our approach lies in the fact that several previously published restoration formulations become special cases of our framework. As a consequence, such methods can be reconsidered by augmenting them with an additional regularization.

The experiments focused on the problem of audio declipping as a natural use case of the proposed framework, where degraded signal samples are constrained to exceed a known clipping level. We have demonstrated the applicability of the regularized AR method and conducted a comparison with current state-of-the-art methods. We have proven the competitiveness of the proposed solution in declipping of

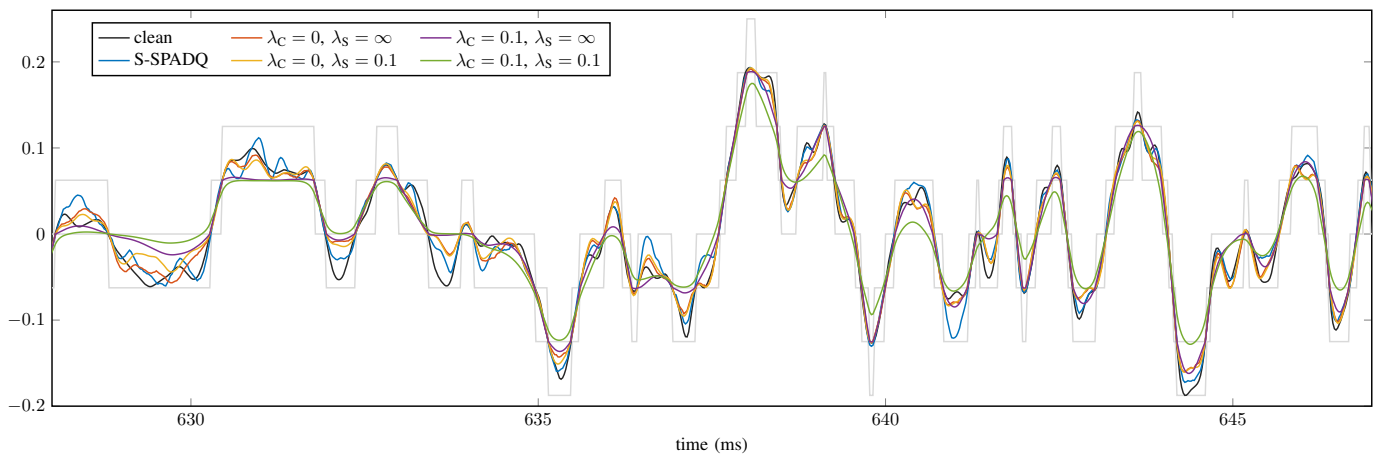


Fig. 7. Audio dequantization experiment, piano, 5-bit quantization. Each sample is constrained by the nearest decision levels, shown by the gray lines.

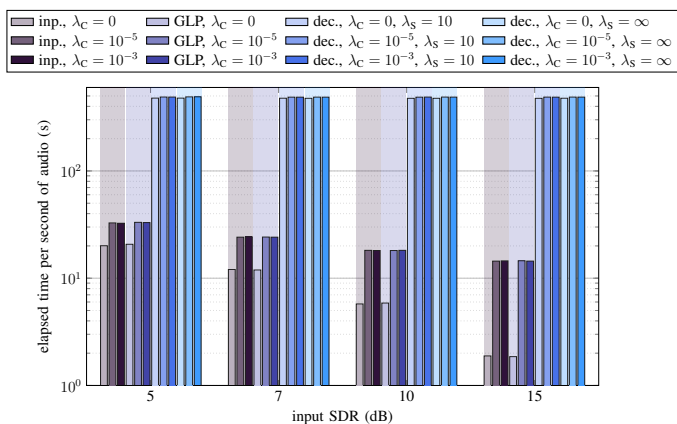


Fig. 8. Elapsed times of the AR-based methods in the declipping experiment from Sec. IV-D and Fig. 4.

music, and we have shown its superiority in declipping on a speech dataset.

We have also pointed out the main drawback of the regularized AR modeling, which is the computational complexity. In the presented declipping application, this was mainly due to the choice of rather large dimensionality of both the coefficient and signal domains of the central problem (16). While we have proposed several strategies allowing a substantial reduction of the computational times, further acceleration for audio processing applications remains a challenge.

Regarding other future directions, the relationship of the AR coefficients and the signal, invoked by the minimization (9), could be relaxed such that the noise (error) is shaped according to the masking properties of the human ear [2, Sec. 4.1]. Such modification could lead to a higher perceptual quality of the solution when using the proposed AR framework in the reconstruction of degraded audio signals.

APPENDIX A ACCELERATION

This appendix presents different strategies to accelerate the solution to the problem (16), following section III-B. Two different approaches are presented in sections A-A and A-B and evaluated numerically in section A-C.

A. Progressive sub-iteration counts

Inspired by the trade-off behavior between outer and inner iteration counts (see Sec. IV-A and Fig. 2), we propose a progressive strategy of choosing the inner iteration counts. Since it appears from the experiments that high precision is necessary for a satisfactory estimation in a single outer iteration, the idea is to “spare” some inner iterations only in the beginning of the ACS while keeping the necessary precision in the final iterations, where the resulting signal is sought. More specifically, a logarithmic distribution of the inner iterations is proposed. Denote I the number of outer iterations and $N^{(i)}$ the number of inner iterations for $i = 1, \dots, I$. For the chosen values of $n^{(1)}$ and $n^{(I)}$, the proposed scheme is

$$N^{(i)} = 10^{n^{(1)} + \frac{i-1}{I-1}(n^{(I)} - n^{(1)})}, \quad (18)$$

or, in Matlab notation²,

$$[N^{(1)}, \dots, N^{(I)}] = \text{logspace}(n^{(1)}, n^{(I)}, I). \quad (19)$$

In particular, it holds $N^{(1)} = 10^{n^{(1)}}$ and $N^{(I)} = 10^{n^{(I)}}$.

B. Extrapolation and line search in the sub-problems

Although the acceleration of DRA helps to significantly reduce the computational time, especially in the signal-estimation sub-problem, the whole ACS algorithm remains very demanding. As outlined in Sec. IV-A, the reason is that an accurate solution of the sub-problems is necessary to achieve satisfactory results of the ACS algorithm.

In response to this observation, we propose several extrapolation strategies for the sub-problems, as well as for the whole ACS:

1) **extrapolate the coefficient update:**

- compute $\mathbf{a}^{(i-\frac{1}{2})}$ as a solution to (14a),
- extrapolate $\mathbf{a}^{(i)} = (1 + \tau_C)\mathbf{a}^{(i-\frac{1}{2})} - \tau_C\mathbf{a}^{(i-1)}$ for the chosen step size $\tau_C > 0$,

2) **extrapolate the signal update:**

- compute $\mathbf{x}^{(i-\frac{1}{2})}$ as a solution to (14b),

²<https://www.mathworks.com/help/matlab/ref/logspace.html>

- extrapolate $\mathbf{x}^{(i)} = (1 + \tau_S)\mathbf{x}^{(i-\frac{1}{2})} - \tau_S\mathbf{x}^{(i-1)}$ for the chosen step size $\tau_S > 0$,

3) line search:

- compute $\mathbf{a}^{(i-\frac{1}{2})}$ as a solution to (14a),
- compute $\mathbf{x}^{(i-\frac{1}{2})}$ as a solution to (14b) with $\mathbf{a}^{(i-\frac{1}{2})}$ fixed instead of $\mathbf{a}^{(i)}$,
- choose $\hat{\tau}$ such that

$$\hat{\tau} = \arg \min_{\tau \geq 0} Q(\mathbf{a}(\tau), \mathbf{x}(\tau)), \quad (20)$$

where $\mathbf{a}(\tau) = (1 + \tau)\mathbf{a}^{(i-\frac{1}{2})} - \tau\mathbf{a}^{(i-1)}$
and $\mathbf{x}(\tau) = (1 + \tau)\mathbf{x}^{(i-\frac{1}{2})} - \tau\mathbf{x}^{(i-1)}$,

- extrapolate as $\mathbf{a}^{(i)} = \mathbf{a}(\hat{\tau})$ and $\mathbf{x}^{(i)} = \mathbf{x}(\hat{\tau})$.

A problem of the line search strategy is the non-convexity³ of the composed problem (12). Thus, no guarantee of finding a minimum with respect to the considered half-line is at hand in general. However, our empirical examples show that an improvement of the objective via sampling a suitable selection of the half-line is possible.

C. Numerical experiment

The acceleration strategies proposed above have been tested on a declipping problem with an input SDR of 10 dB (see Sec. IV for details). As the baseline serves the ACS algorithm with $I = 10$ outer iterations and DRA as the sub-solver with 1 000 iterations. The accelerated versions include:

- FFT-based acceleration of the DRA [45].
- Progressive iteration according to Sec. A-A with 100 iterations of DRA in the first iteration of ACS ($n^{(1)} = 2$, $N^{(1)} = 100$) and 1 000 iterations of DRA in the last iteration of ACS ($n^{(10)} = 3$, $N^{(10)} = 1 000$), spaced logarithmically.
- Extrapolation according to Sec. A-B with the following extrapolation steps for the signal and/or the AR model coefficients in the iteration i of $I = 5$:

$$\mathbf{x}^{(i)} = \mathbf{x}^{(i-\frac{1}{2})} + \frac{I-i}{I-1}(\mathbf{x}^{(i-\frac{1}{2})} - \mathbf{x}^{(i-1)}), \quad (21a)$$

$$\mathbf{a}^{(i)} = \mathbf{a}^{(i-\frac{1}{2})} + 2\frac{I-i}{I-1}(\mathbf{a}^{(i-\frac{1}{2})} - \mathbf{a}^{(i-1)}). \quad (21b)$$

In line with A-B, we have in the i -th iteration $\tau_S = \frac{I-i}{I-1}$ (i.e., the extrapolation step length decreases from $\tau_S = 1$ in the first iteration to $\tau_S = 0$, meaning no extrapolation in the I -th iteration). Similarly, we have $\tau_C = 2\frac{I-i}{I-1}$.

- Line search according to Sec. A-B, considering only $\tau \in [0.0001, 100]$ for computational reasons.

To evaluate the acceleration, the computation time is tracked for the considered ways of estimating the AR coefficients and the declipped signal, together with the reconstruction quality. The experiment was performed on a PC with the Intel Core i7 3.40 GHz processor, 32 GB RAM.

The numerical results for five short signals⁴ are presented in Fig. 9 and 11. Fig. 9 shows the individual reconstructions

³In the context of the line search, an important observation is that the objective is non-convex over the half-line under consideration. The only exception is a discrete set of search directions, as can be observed in an illustrative example of $Q(a, x) = a \cdot x$ with the scalars a, x .

⁴The test signals are single-instrument recordings extracted from the set based on the EBU SQAM database, as described in Sec. IV, and shortened to a length of 0.6 s.

in the time-quality plane, where the reconstruction quality is measured using SDR. In this plot, a suitable acceleration strategy should have its data points to the left from the baseline (meaning lower computational time) and not below the baseline (meaning the same or a better reconstruction quality). The same data are shown in Fig. 11 in a different manner. There, the decrease in computational time (i.e., time gain) and decrease in SDR (i.e., performance loss) are shown together as stacked bars for each acceleration strategy. Furthermore, this plot shows the data for different orders of the AR model and different frame lengths, since the acceleration rate is supposed to depend on the problem size. Note that all the values shown in Fig. 11 are relative with respect to the baseline values shown in Fig. 10.

The conclusion from this experiment is that the most beneficial option is to use the FFT-accelerated DRA in both sub-problems of (14). The computation time is greater merely in some cases of inpainting and GLP. Regarding the reconstruction quality, the PEAQ ODG values do not show any difference, and the related graphical representation is thus omitted. In terms of PEAQ ODG or SDR, a loss of reconstruction quality is observed; mainly in cases including the extrapolation of the estimated AR model. A less significant quality loss is observed in the line search case and signal extrapolation.

As a compromise between acceleration and reconstruction quality loss, the experiment favors using 1 000 inner iterations of the FFT-accelerated DRA with extrapolation of the signal update according to (21a) (see Fig. 9 and 11).

APPENDIX B DECLIPPED SIGNAL CONSISTENCY

While the proposed signal regularization rationalizes the use of AR model for audio declipping, the results do not show large improvement over the inpainting or GLP techniques in many cases. A hypothesis is that although consistency in the time domain (satisfying the clipping conditions) can be approached with $\lambda_S > 0$ and even theoretically guaranteed in the case of $\lambda_S = \infty$, solving the sub-problem (14b) in an iterative manner carries the risk of reaching only an approximate solution. Furthermore, consistency does not necessarily ensure higher SDR.

To support these ideas, we analyze the resulting signals from the experiment presented in Sec. IV-D and relate the Δ SDR scores (see also Eq. (17)) to the consistency of the signals. For any solution $\hat{\mathbf{x}}$, we measure the (squared) distance from the consistency set $\frac{1}{2}d_{\Gamma_{\text{declip}}}(\hat{\mathbf{x}})^2 = \frac{1}{2}\|\hat{\mathbf{x}} - \text{proj}_{\Gamma_{\text{declip}}}(\hat{\mathbf{x}})\|^2$, which is also part of the objective of the problem (16) in the declipping case. The assorted results for all audio samples and all values of input SDR are shown in Fig. 12.

Importantly, GLP reaches similar values of $d_{\Gamma_{\text{declip}}}(\hat{\mathbf{x}})^2$ compared to inpainting, which means that in our experiments, the heuristic signal rectification step in GLP does not guarantee consistency of the result. On the other hand, the declipping strategy provides solutions that tend towards lower values of $d_{\Gamma_{\text{declip}}}(\hat{\mathbf{x}})^2$, approaching even (numerical) zero in the case of $\lambda_S = \infty$.

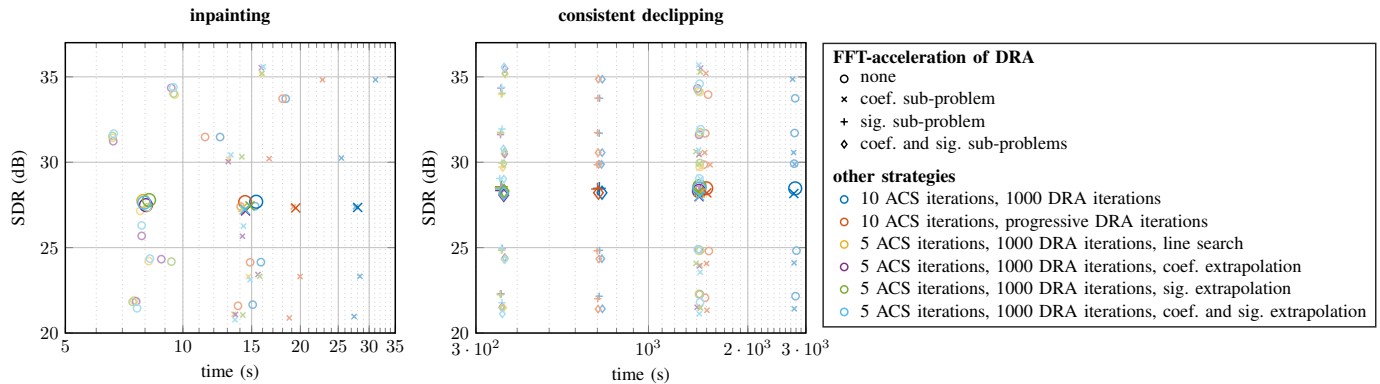


Fig. 9. Comparison of the acceleration options for the frame length $w = 8192$ samples and the AR model order $p = 512$. The smaller and lighter points represent individual reconstructions in the experiment, the larger points are the mean values.

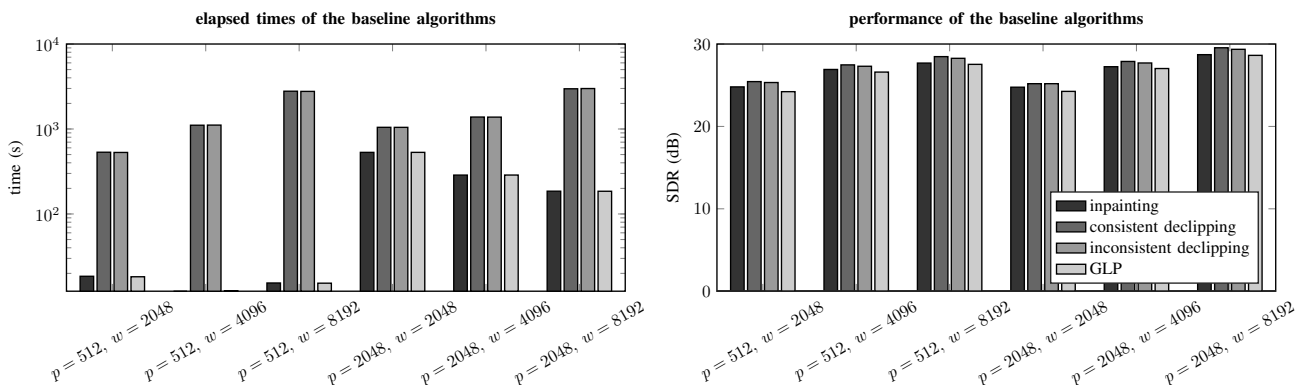


Fig. 10. Baseline elapsed times and performance in terms of SDR using 10 ACS iterations and 1000 DRA iterations with no acceleration strategy.

Regarding the relation of consistency and reconstruction quality, Fig. 12 reveals some correlation in the case of inpainting and GLP. This is natural in the sense that very high SDR values correspond to the solution $\hat{\mathbf{x}}$ being close to the ground truth signal, which is necessarily consistent. In the declipping case, (approximate) consistency was ensured by definition of the problem, thus no further correlation with ΔSDR is observed.

APPENDIX C

ELAPSED TIMES IN A DEMONSTRATIVE EXAMPLE

Fig. 13 shows an illustrative example on the computation times, depending on several parameters. The reconstruction task concerns a single realization of an AR process of length N samples which was peak-normalized and clipped depending on the threshold θ_{clip} . Different variants of the ACS algorithm are employed (using 1000 inner iterations of the FFT-accelerated DRA), as in Sec. IV, and elapsed time is measured.

The plots illustrate in more detail several expected facts, following up on Sec. IV-G and also extending the results in Fig. 8 and 10:

- The declipping task is numerically more demanding than either inpainting or GLP, independent of the value of λ_S .
- The regularization of the AR coefficients makes the estimation more demanding compared to standard methods like the Levinson–Durbin algorithm.

- The complexity grows with the model order (see the first plot in Fig. 13) and signal/window length (second plot in Fig. 13).
- The clipping threshold (or number of missing samples) only affects the complexity of the inpainting and GLP methods. The load grows with the number of missing samples, i.e., it decreases with θ_{clip} (see the third plot in Fig. 13).

APPENDIX D

PROXIMAL OPERATORS

In this appendix, we treat in more detail the components utilized to fit the proposed regularized AR model in the case of audio declipping, i.e., to solve the problem (16). In (15), we already have introduced the proximal operators of the error term appearing in (16). For the sparsity term $\tau\|\mathbf{a}\|_1$ with any scalar $\tau > 0$, the corresponding proximal operator $\text{prox}_{\tau\|\cdot\|_1}$ is the soft thresholding with a threshold of τ [44, Ex. 6.8]:

$$\left(\text{prox}_{\tau\|\cdot\|_1}(\mathbf{a})\right)_n = \begin{cases} a_n - \tau, & a_n \geq \tau, \\ 0, & |a_n| < \tau, \\ a_n + \tau, & a_n \leq -\tau. \end{cases} \quad (22)$$

Regarding the signal regularization $\tau d_{\Gamma_{\text{declip}}}(\mathbf{x})^2/2$, we have for $\tau < \infty$ [44, Ex. 6.65]

$$\text{prox}_{\tau d_{\Gamma_{\text{declip}}}(\mathbf{x})^2/2}(\mathbf{x}) = \frac{\tau}{\tau+1} \text{proj}_{\Gamma_{\text{declip}}}(\mathbf{x}) + \frac{1}{\tau+1} \mathbf{x}. \quad (23)$$

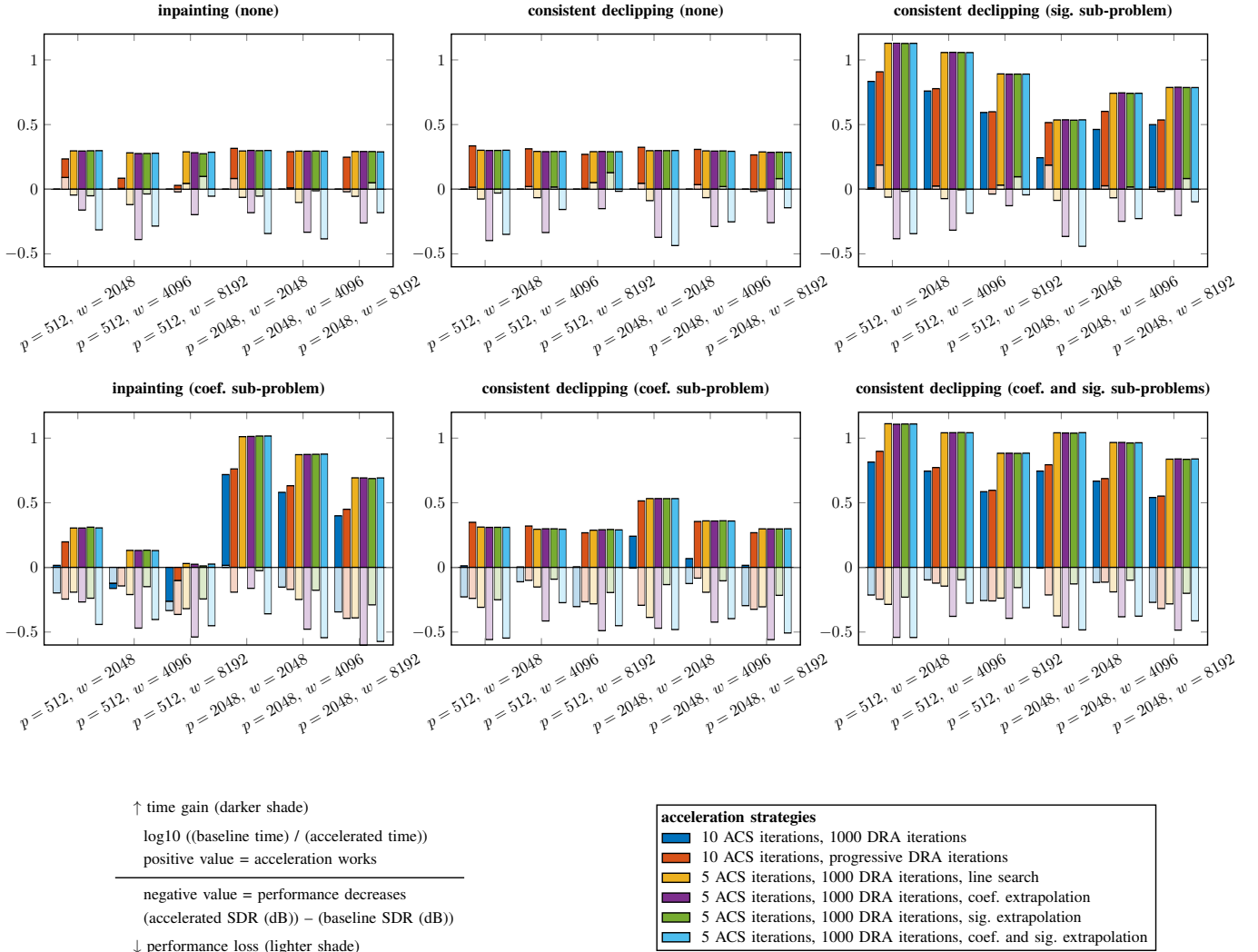


Fig. 11. Performance of the acceleration strategies for an input SDR of 10 dB, dependent on the frame length w and the AR model order p . Color coding is the same in the whole figure and is identical to Fig. 9. FFT-acceleration of the DRA in the coefficient and signal sub-problems (14a) and (14b) is indicated in brackets above the individual plots. Positive time gain (darker-shade bar has a value above 0) means that the acceleration truly reduces computation time. A positive performance loss (the lighter-shade bar has a value below 0) means that the acceleration causes a drop in the reconstruction SDR. For the baseline time and SDR, see Fig. 10.

To cover also the consistent case with $\mathbf{x} \in \Gamma_{\text{declip}}$, we allow the choice $\tau = \infty$, which is interpreted as replacing $\tau d_{\Gamma_{\text{declip}}}(\mathbf{x})^2/2$ with the indicator function $\iota_{\Gamma_{\text{declip}}}(\mathbf{x})$. The corresponding proximal operator is the projection [44, Thm. 6.24]

$$\text{prox}_{\iota_{\Gamma_{\text{declip}}}}(\mathbf{x}) = \text{proj}_{\Gamma_{\text{declip}}}(\mathbf{x}). \quad (24)$$

While (24) is the limit case of (23) for $\tau \rightarrow \infty$, our Matlab implementation treats the two cases individually.

ACKNOWLEDGMENT

The work was supported by the Czech Science Foundation (GAČR) Project No. 23-07294S.

REFERENCES

- [1] U. Zölzer, *DAFX: Digital Audio Effects*, 2nd ed., U. Zölzer, Ed. Wiley, 2011.
- [2] A. Spanias, T. Painter, and V. Atti, *Audio Signal Processing and Coding*. John Wiley & Sons, Inc., 12 2005.
- [3] R. S. Tsay, *Analysis of financial time series*, 2nd ed. Hoboken, New Jersey: Wiley, 2005.
- [4] H. Akaike, *Autoregressive Model Fitting for Control*. New York, NY: Springer New York, 1998, pp. 153–170. [Online]. Available: https://doi.org/10.1007/978-1-4612-1694-0_12
- [5] T. Takahashi, K. Konishi, and T. Furukawa, “Hankel structured matrix rank minimization approach to signal declipping,” in *21st European Signal Processing Conference (EUSIPCO 2013)*, Sep. 2013, pp. 1–5.
- [6] P. Závíška, P. Rajmic, and O. Mokry, “Multiple Hankel matrix rank minimization for audio inpainting,” in *2023 46th International Conference on Telecommunications and Signal Processing (TSP)*. IEEE, Jul. 2023.
- [7] W. Eter, “Restoration of a discrete-time signal segment by interpolation based on the left-sided and right-sided autoregressive parameters,” *IEEE Transactions on Signal Processing*, vol. 44, no. 5, pp. 1124–1135, 1996.
- [8] S. Kitić, L. Jacques, N. Madhu, M. Hopwood, A. Priet, and C. De Vleeschouwer, “Consistent iterative hard thresholding for signal declipping,” in *Acoustics, Speech and Signal Processing (ICASSP), 2013 IEEE International Conference on*, May 2013, pp. 5939–5943.
- [9] P. Závíška, P. Rajmic, A. Ozerov, and L. Rencker, “A survey and an extensive evaluation of popular audio declipping methods,” *IEEE*

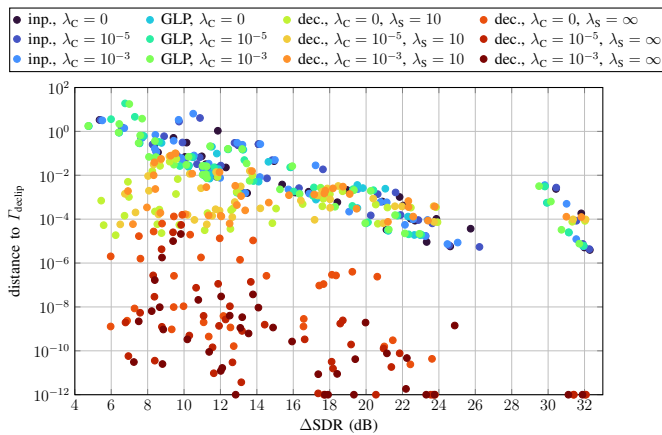


Fig. 12. Consistency of the resulting signals from the experiment from Sec. IV-D and Fig. 4. Note that the values are cropped at the minimal value of 10^{-12} , considered to be essentially zero.

Journal of Selected Topics in Signal Processing, vol. 15, no. 1, pp. 5–24, 2021.

- [10] P. Závřiška, P. Rajmic, and O. Mokřý, “Audio declipping performance enhancement via crossfading,” *Signal Processing*, vol. 192, p. 108365, 2022. [Online]. Available: <https://www.sciencedirect.com/science/article/pii/S0165168421004023>
- [11] P. Závřiška, P. Rajmic, and O. Mokřý, “Audio dequantization using (co)sparse (non)convex methods,” in *2021 IEEE International Conference on Acoustics, Speech and Signal Processing (ICASSP)*, Toronto, Canada, Jun. 2021, pp. 701–705.
- [12] *Pulse code modulation (PCM) of voice frequencies*, Geneva, 1988, ITU-Recommendation G.711.
- [13] A. J. E. M. Janssen, R. N. J. Veldhuis, and L. B. Vries, “Adaptive interpolation of discrete-time signals that can be modeled as autoregressive processes,” *IEEE Trans. Acoustics, Speech and Signal Processing*, vol. 34, no. 2, pp. 317–330, Apr. 1986.
- [14] L. Oudre, “Interpolation of missing samples in sound signals based on autoregressive modeling,” *Image Processing On Line*, vol. 8, pp. 329–344, Oct. 2018.
- [15] O. Mokřý and P. Rajmic, “Audio inpainting: Revisited and reweighted,” *IEEE/ACM Transactions on Audio, Speech, and Language Processing*, vol. 28, pp. 2906–2918, 2020.
- [16] O. Mokřý and P. Rajmic, “Tweaking autoregressive methods for inpainting of gaps in audio signals,” in *2025 33rd European Signal Processing Conference (EUSIPCO)*, 2025, pp. 311–315.
- [17] L. Atlas and P. Clark, “Clipped-waveform repair in acoustic signals using generalized linear prediction,” U.S. patentus US 8 126 578 B2, Sep. 26, 2012. [Online]. Available: <https://patents.google.com/patent/US8126578>
- [18] I. Kauppinen and J. Kauppinen, “Reconstruction method for missing or damaged long portions in audio signal,” *Journal of the Audio Engineering Society*, vol. 50, no. 7/8, pp. 594–602, 2002. [Online]. Available: <http://www.aes.org/e-lib/browse.cfm?elib=11068>
- [19] I. Kauppinen and K. Roth, “Audio Signal Extrapolation – Theory and Applications,” in *Proceedings of the 5th International Conference on Digital Audio Effects (DAFx-02)*, Hamburg, Germany, Sep. 2002, pp. 105–110. [Online]. Available: http://www2.hsu-hh.de/ant/dafx2002/papers/DAFX02_Kauppinen_Roth_signal_extrapolation.pdf
- [20] P. A. A. Esquef, V. Välimäki, K. Roth, and I. Kauppinen, “Interpolation of long gaps in audio signals using the warped Burg’s method,” in *Proceedings of the 6th International Conference on Digital Audio Effects (DAFx-03)*, London, UK, Sep. 2003, pp. 18–23.
- [21] K. Roth, I. Kauppinen, P. A. A. Esquef, and V. Välimäki, “Frequency warped Burg’s method for AR-modeling,” in *2003 IEEE Workshop on Applications of Signal Processing to Audio and Acoustics*, ser. ASPAA-03. IEEE, 2003.
- [22] V. Vesely and J. Tonner, “Sparse parameter estimation in overcomplete time series models,” *Austrian Journal of Statistics*, vol. 35, pp. 371–378, 2006. [Online]. Available: <http://www.stat.tugraz.at/AJS/ausg062+3/062Vesely.pdf>
- [23] D. Giacobello, M. G. Christensen, J. Dahl, S. H. Jensen, and M. Moonen, “Joint estimation of short-term and long-term predictors in speech coders,” in *2009 IEEE International Conference on Acoustics, Speech and Signal Processing*. IEEE, Apr. 2009.
- [24] D. Giacobello, M. G. Christensen, M. N. Murthi, S. H. Jensen, and M. Moonen, “Sparse linear prediction and its applications to speech processing,” *IEEE Transactions on Audio, Speech, and Language Processing*, vol. 20, no. 5, pp. 1644–1657, Jul. 2012.
- [25] B. D. Dufera, K. Eneman, and T. van Waterschoot, “Missing sample estimation based on high-order sparse linear prediction for audio signals,” in *2018 26th European Signal Processing Conference (EUSIPCO)*. IEEE, Sep. 2018.
- [26] B. D. Dufera, E. Adugna, K. Eneman, and T. van Waterschoot, “Restoration of click degraded speech and music based on high order sparse linear prediction,” in *2019 IEEE AFRICON*. IEEE, Sep. 2019.
- [27] P. T. Troughton, “Bayesian restoration of quantised audio signals using a sinusoidal model with autoregressive residuals,” in *Proceedings of the 1999 IEEE Workshop on Applications of Signal Processing to Audio and Acoustics*, Oct. 1999, pp. 159–162.
- [28] P. T. Troughton and S. J. Godsill, “MCMC methods for restoration of quantised time series,” in *Proceedings of the IEEE-EURASIP Workshop on Nonlinear Signal and Image Processing (NSIP’99)*. Bogaziçi University Printhouse, 1999, pp. 447–451.
- [29] —, “MCMC methods for restoration of nonlinearly distorted autoregressive signals,” *Signal Processing*, vol. 81, no. 1, pp. 83–97, Jan. 2001.
- [30] T. Tanaka, K. Yatabe, M. Yasuda, and Y. Oikawa, “APPLADE: Adjustable plug-and-play audio declipper combining DNN with sparse optimization,” in *2022 IEEE International Conference on Acoustics, Speech and Signal Processing (ICASSP)*. IEEE, May 2022.
- [31] Y. Kwon and J.-W. Choi, “Speech-declipping transformer with complex spectrogram and learnable temporal features,” 2024. [Online]. Available: <https://arxiv.org/abs/2409.12416>
- [32] V. Sechaud, L. Jacques, P. Abry, and J. Tachella, “Equivariance-based self-supervised learning for audio signal recovery from clipped measurements,” 2024. [Online]. Available: <https://arxiv.org/abs/2409.15283>
- [33] M. Švento, P. Rajmic, and O. Mokřý, “Plug-and-play audio restoration with diffusion denoiser,” in *2024 18th International Workshop on Acoustic Signal Enhancement (IWAENC)*, vol. 1. IEEE, Sep. 2024, pp. 115–119. [Online]. Available: <https://ieeexplore.ieee.org/document/10694642>
- [34] A. van den Oord, S. Dieleman, H. Zen, K. Simonyan, O. Vinyals, A. Graves, N. Kalchbrenner, A. Senior, and K. Kavukcuoglu, “WaveNet: A generative model for raw audio,” in *Proc. 9th ISCA Workshop on Speech Synthesis Workshop (SSW 9)*, 2016.
- [35] O. Triebe, N. Laptev, and R. Rajagopal, “AR-Net: A simple autoregressive neural network for time-series,” 2019. [Online]. Available: <https://arxiv.org/abs/1911.12436>
- [36] A. I. Mezza, M. Amerena, A. Bernardini, and A. Sarti, “Hybrid packet loss concealment for real-time networked music applications,” *IEEE Open Journal of Signal Processing*, vol. 5, pp. 266–273, 2024.
- [37] P. J. Brockwell and R. A. Davis, *Time Series: Theory and Methods*, 2nd ed., ser. Springer series in statistics. Springer, 2006.
- [38] J. Durbin, “The fitting of time-series models,” *Revue de l’Institut International de Statistique / Review of the International Statistical Institute*, vol. 28, no. 3, p. 233, 1960.
- [39] N. Levinson, “The Wiener (root mean square) error criterion in filter design and prediction,” *Journal of Mathematics and Physics*, vol. 25, no. 1–4, pp. 261–278, Apr. 1946.
- [40] M. Aharon, M. Elad, and A. M. Bruckstein, “K-SVD: An algorithm for designing of overcomplete dictionaries for sparse representations,” *IEEE Transactions on Signal Processing*, vol. 54, pp. 4311–4322, 2006.
- [41] J. Gorski, F. Pfeuffer, and K. Klamroth, “Biconvex sets and optimization with biconvex functions: a survey and extensions,” *Mathematical Methods of Operations Research*, vol. 66, no. 3, pp. 373–407, Jun. 2007.
- [42] P. L. Combettes and J.-C. Pesquet, “Proximal splitting methods in signal processing,” *Fixed-Point Algorithms for Inverse Problems in Science and Engineering*, vol. 49, pp. 185–212, 2011.
- [43] P. Jain and P. Kar, *Non-convex Optimization for Machine Learning*. now publishers inc., 2017. [Online]. Available: <https://www.nowpublishers.com/article/Details/MAL-058>
- [44] A. Beck, *First-Order Methods in Optimization*. SIAM-Society for Industrial and Applied Mathematics, 2017.
- [45] I. Bayram, “Proximal mappings involving almost structured matrices,” *IEEE Signal Processing Letters*, vol. 22, no. 12, pp. 2264–2268, Dec. 2015.
- [46] A. Adler, V. Emiya, M. G. Jafari, M. Elad, R. Gribonval, and M. D. Plumbley, “Audio inpainting,” *IEEE Transactions on Audio, Speech, and Language Processing*, vol. 20, no. 3, pp. 922–932, Mar. 2012.

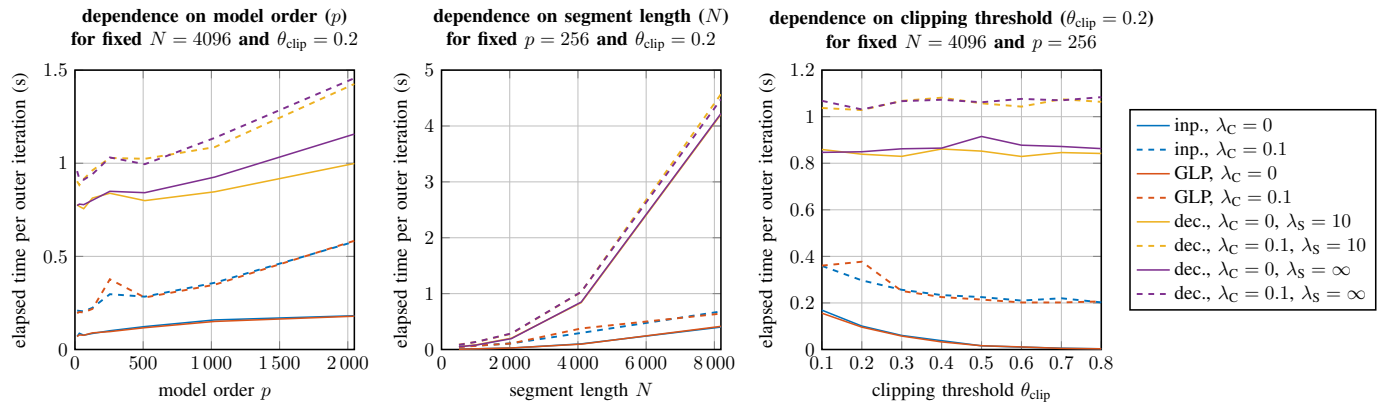


Fig. 13. Elapsed times for declipping on a single frame of a realization of an AR process.

- [47] R. Huber and B. Kollmeier, "PEMO-Q—A new method for objective audio quality assessment using a model of auditory perception," *IEEE Trans. Audio Speech Language Proc.*, vol. 14, no. 6, pp. 1902–1911, Nov. 2006.
- [48] T. Thiede, W. C. Treurniet, R. Bitto, C. Schmidmer, T. Sporer, J. G. Beerends, C. Colomes, M. Keyhl, G. Stoll, K. Brandenburg, and B. Feiten, "PEAQ – The ITU standard for objective measurement of perceived audio quality," *Journal of the Audio Engineering Society*, vol. 48, no. 1/2, pp. 3–29, January/February 2000. [Online]. Available: <http://www.aes.org/e-lib/browse.cfm?elib=12078>
- [49] P. Kabal, "An examination and interpretation of ITU-R BS.1387: Perceptual evaluation of audio quality," MMSP Lab, Dept. Electrical & Computer Engineering, McGill University, Tech. Rep., May 2002. [Online]. Available: <https://www-mmsp.ece.mcgill.ca/Documents/Reports/2002/KabalR2002v2.pdf>
- [50] "EBU SQAM CD: Sound quality assessment material recordings for subjective tests," 2008. [Online]. Available: <https://tech.ebu.ch/publications/sqamcd>
- [51] M. Hollander and D. A. Wolfe, *Nonparametric statistical methods*, 2nd ed., ser. Wiley series in probability and statistics. Texts and references section. New York: John Wiley & Sons, 1999.
- [52] C. Valentini-Botinhao, "Noisy speech database for training speech enhancement algorithms and tts models," 2017. [Online]. Available: <https://datashare.ed.ac.uk/handle/10283/2791>
- [53] C. H. Taal, R. C. Hendriks, R. Heusdens, and J. Jensen, "A short-time objective intelligibility measure for time-frequency weighted noisy speech," in *2010 IEEE International Conference on Acoustics, Speech and Signal Processing*. IEEE, 2010.
- [54] —, "An algorithm for intelligibility prediction of time-frequency weighted noisy speech," *IEEE Transactions on Audio, Speech, and Language Processing*, vol. 19, no. 7, pp. 2125–2136, Sep. 2011.
- [55] A. Hines, J. Skoglund, A. Kokaram, and N. Harte, "Visqol: an objective speech quality model," *EURASIP Journal on Audio, Speech, and Music Processing*, vol. 13, no. 1, pp. 1–18, May 2015.
- [56] M. Chinen, F. S. C. Lim, J. Skoglund, N. Gureev, F. O’Gorman, and A. Hines, "Visqol v3: An open source production ready objective speech and audio metric," in *2020 Twelfth International Conference on Quality of Multimedia Experience (QoMEX)*. IEEE, May 2020.
- [57] A. Hines and N. Harte, "Speech intelligibility prediction using a neurogram similarity index measure," *Speech Communication*, vol. 54, no. 2, pp. 306–320, Feb. 2012.